Blow-up regimes by non-isothermal gas/steam filtration through the underground particle layer with internal heat sources

Ivan V. Kazachkov
ivan.kazachkov@energy.kth.se

Abstract—Two-dimensional non-stationary model for the non-isothermal gas/steam filtration through a monospherical particle layer with internal heat generation is considered with a particular emphasis on the non-thermal gas/particles local equilibrium, taking into account the real non-linear properties of the media. The boundary problem for the multiphase system of gas and particles is formulated and solved numerically using the effective finite-difference fractional time-step method. It is shown that some initial thermodynamic perturbations in the system may cause localization of a gas heating (mainly due to a non-linear heat conductivity), which will lead to a temperature escalation in a specific spatial subdomains. Furthermore, the effects of other parameters such as particles' size and porosity of the layer, an amplitude and a form of an initial temperature perturbation, the level of an initial temperature difference between the gas and solid phases, etc. are analyzed.

The model considered can be comparably easily modified for the three-dimensional non-stationary case using the numerical algorithm applied. An examples of computer simulations are presented for the cases of the volcanic geological mains and for the nuclear power safety. The phenomenon of the blow-up regimes due to non-linear heat conductivity causing local abnormal heat escalation in a narrow domain may be of great interest for some natural, as well as technical systems and processes.

Keywords—Blow-up heating, filtration, underground layer, non-linear heat conductivity.

I. Introduction

The problem of a non-stationary non-isothermal gas (steam) flow in porous media with account of the real physical properties of the media, which can strongly depend on the temperature spatial distribution, is of paramount interest for a lot of modern industrial, technological and natural processes, for example the following ones:

- Coolability of a heat-generating porous beds in a severe accidents at the Nuclear Power Plants [1, 2]
- Gas and steam flow through the underground permeable layers in Geothermal and Gas Industry as well as Vulcanology [3, 4]
- Diverse gas and steam flows in Chemical Reactors, porous elements of the Avionic Components, etc. [5, 6].

An early theoretical and experimental study of the thermal hydraulics in a volumetrically heated porous layer is that of Choudhary and El-Wakil [7] who solved numerically the linear energy equation for the solid and gas mixture by an implicit modified Crank-Nicolson method. Vasiliev and Mairov [8] analyzed heat transfer, pressure drop and stability characteristics of a volumetrically heated porous layer cooled with forced flow evaporation.

Depending on the physical properties of the coolant, they divided the porous layer into three regions: subcooled, saturated two phase mixture and superheated steam.

The energy equations with appropriate boundary conditions were solved for each region to obtain the temperature distribution in a solid and a fluid phases. Later, Naik and Dhir [9] experimentally investigated a volumetrically heated porous layer and obtained the data for the steady state temperature profile and pressure drop of an evaporating two-phase coolant flowing vertically. The one-dimensional energy equations for the particles and coolant with assumption of no differences between the solid and liquid temperatures, were solved. The two-phase pressure drop was evaluated by a separated flow model using the experimental data and the void fraction was correlated as a function of the flow regime and mass flow rate. The model showed reasonable correlation for a water-steam flow at atmospheric pressure but not as well for the fluid mixtures with a higher vapor/liquid volume ratio.

Hofmann [10] presented the experimental and analytical investigation on dryout heat flux in inductively heated beds for the both top and top-and-bottom fed conditions considering the heat flux as a function of a saturation by solving the mass, momentum and energy conservation equations. But no satisfactory correlation with experimental data was achieved. Several experimental and analytical studies on hydrodynamic aspects of two-phase flow through porous media were summarized by Schulenberg and Mueller [11].

Unfortunately these studies were mostly done for a one-dimensional homogeneous porous layer, whereas those encountered in actual practice are multi-dimensional and often with varying permeabilities and heating conditions.

Tsai [12] measured dryout heat fluxes in axisymmetric porous layers with partial volumetric heating. But his numerical solution obtained with "pseudo stream functions" exists only for a certain distribution of a volumetric heating in the porous layers.

The hydrodynamic model by Tung and Dhir [13] predicts void fractions and pressure gradient for one-dimensional

two-phase flow in porous media with a particle-gas, particle-liquid and liquid-gas interfacial drag evaluated for the different flow regimes. This mechanistic model was then modified and solved numerically [14]. The numerical finite element model allowed the existence of several subdomains with different permeabilities. A multi-dimensional mathematical model was developed by Stubos and Buchlin [15] assuming a local thermal equilibrium between the solid and liquid phases, which may not be satisfactory for the early stages of the transport processes when the fluid and particle temperatures differ. This is also important during the later stages of the transport processes in high speed flows in which the fluid-solid interaction time is not enough to bring the temperatures of the phases to equilibrium state.

II. STATEMENT OF THE PROBLEM

A. Non-thermal equilibrium flow in a porous medium

Non-thermal equilibrium flow through a porous medium is of special interest. Nigmatulin [16] derived the equations of a saturated monospherical particle layer in a heterogeneous non-thermal equilibrium approach, with account of the deformable properties of the layer. Based on his equations, two-dimensional mathematical model and numerical algorithm were developed by Kazachkov [4] for the steam flow in a particle layer surrounded by the impermeable medium. The model was applied for the numerical simulation of a non-stationary non-isothermal filtration in geothermal systems.

Kazachkov and Konovalikhin [1] modified the model to describe the dryout location by introducing the initial thermodynamic perturbations, which may lead to abnormal temperature escalation in a local subdomain. An analysis of the steam thermal behavior in the two-dimensional homogeneous and stratified porous beds with temperature dependent thermal conductivity has been performed, which revealed the reasonable agreement of the model with experimental data.

B. Other non-thermal equilibrium models

Sözen and Vafai [17] presented a general set of the volume-averaged governing equations for the non-thermal equilibrium condensing forced flow through a latent heat storage porous media. And a comprehensive numerical study of the phenomenon has been carried out.

Kuznetsov [18] has performed analysis based on solution, by the perturbation technique, of the full energy equations for incompressible fluid and solid phases. He showed that the temperature between fluid and solid phases in a semi-infinite packed bed forms a spatially localized wave. Later on, he investigated [19, 20] a thermal behavior of a three-dimensional porous bed in a non-thermal equilibrium flow through it assuming the constant thermal, physical and transport properties.

C. Nuclear power safety problemss

A detail study of a two-dimensional non-stationary non-isothermal gas (steam) filtration through a monospherical particle layer under internal heat generation, with a particular emphasis on the non-thermal gas/particle local equilibrium and a real non-linear properties of the media has been performed both theoretically and experimentally in [1, 2, 4, 21-24].

III. DEVELOPMENT OF THE MODEL EQUATIONS

A. Basic equations

Mathematical model for the numerical simulation of a compressible fluid (gas/steam) flow through the volumetrically heated porous bed with particular consideration of the non-thermal local equilibrium is formulated. Fig. 1 depicts schematically the physical problem considered. A two-dimensional self-heated porous packed bed, which consists of homogeneous spherical particle layer (in general, K monolayers may be considered as well) is filled with a gas (steam), which moves from the bottom to the top, and is initially at the known temperature distribution.

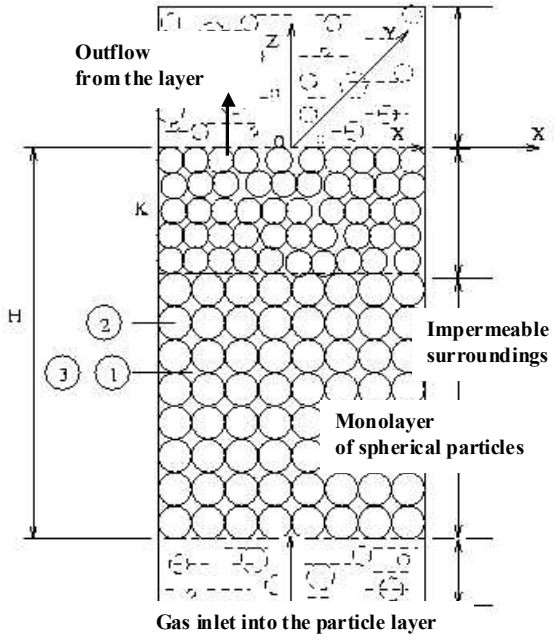

Fig. 1. Structural scheme of the heterogeneous particle-gas media

By a development of the mathematical model, the following assumptions were employed:

- The flow is single phase and is compressible (gas, steam)
- The particles' sizes are significantly larger than molecular-kinetic scales, but they are significantly less than the characteristic scale of the system
- The physical properties of the media such as thermal conductivity, viscosity, density, etc. are temperature dependent
- Solid particles are immovable and porosity is constant in each monolayer.

Based on the equations of the saturated granular layer introduced by Nigmatulin [16] in heterogeneous approach, the mathematical model for the above-described system, presented schematically in Fig.1, was developed by Kazachkov [4] for the mathematical simulation of the non-stationary non-isothermal gas (steam) filtration processes. In a two-

dimensional case, the mathematical model of the gas filtration in a spherical particle monolayer can be presented as follows.

Continuity equation for the compressible gas flow is

$$\frac{\partial \rho_1^0}{\partial t} + \rho_1^0\left(\frac{\partial u_1}{\partial x} + \frac{\partial w_1}{\partial z}\right) + u_1\frac{\partial \rho_1^0}{\partial x} + w_1\frac{\partial \rho_1^0}{\partial z} = 0, \quad (1)$$

Dynamic equilibrium equation for the immovable particles ($\vec{v}_2 = 0$) of the layer and the momentum equation for the gas flow are, respectively:

$$-0.5\alpha_2\rho_1\frac{\partial \vec{v}_1}{\partial t} + \alpha_2\nabla p_1 + \rho_2\vec{g} = \vec{f}_\mu + \nabla \bullet \boldsymbol{\sigma}_k, \quad (2)$$

$$\rho_1^0\alpha_1(1+0.5\alpha_2)\frac{\partial \vec{v}_1}{\partial t} + \alpha_1\nabla p_1 + \rho_1^0\alpha_1\vec{g} = -\alpha_1\vec{f}_\mu, \quad (3)$$

where ρ_1^0 is a gas real density and ρ_1 is its partial density in the heterogeneous mixture, K_0 is a permeability of the layer, ∇ is gradient, $\vec{f}_\mu = \mu_1\frac{\vec{v}_1}{K_0}\left(\frac{\alpha_1}{\alpha_{10}}\right)^{-n}$ and $\boldsymbol{\sigma}_k$ are the interfacial viscous force and the "effective" stress tensor in the layer [16], respectively. Here $\vec{v}_1 = \{u_1, w_1\}$ is gas velocity, which contains the horizontal and vertical components, μ_1 is the gas dynamic viscosity, α_{10} is the porosity of the layer by given temperature T_{10}. Under the assumptions made, the solid particles are immovable and the porosity is constant, so that here must be stated that $\boldsymbol{\sigma}_k = 0$ and $\alpha_1 = \alpha_{10} = const$.

The density of the two-phase mixture is $\rho = \alpha_1\rho_1^0 + \alpha_2\rho_2$, where α_1 is the gas volume component and α_2 is the volume component of particles in the saturated layer. Thus obviously the equation $\alpha_1 + \alpha_2 = 1$ should be satisfied. The other parameters of two-phase system are calculated in a similar way, e.g. temperature of the mixture in the layer is $T = \alpha_1 T_1 + \alpha_2 T_2$. The first, inertial term in the equations (2), (3) is written with account of the associated mass for the spherical particle in a non-stationary flow, and the interfacial viscous force term $\vec{f}_\mu$ expresses the viscous force acting between the particle and gas flow.

The energy conservation equations are written for two phases of the saturated particle layer (for the fluid and particles) and the non-permeable surrounding medium (heat conductive medium) separately:

$$\rho_1 c_{v1}\left(\frac{\partial T_1}{\partial t} + \vec{v}\nabla T_1\right) = \alpha_1 R T_1\frac{\partial \rho_1^0}{\partial t} + \nabla(k_1\nabla T_1) + Q_\Sigma + Q_V + \mu_1(u_1^2 + w_1^2)\frac{\alpha_1}{K}, \quad (4)$$

$$\rho_j c_j\frac{\partial T_j}{\partial t} = \nabla(k_j\nabla T_j) + (j-3)Q_\Sigma, \quad (5)$$

where are: $K = K_0(\alpha_1/\alpha_{10})^n$ - permeability of the layer (here it is constant due to constant porosity), $k_1 = \mu_1 c_{p1}/\mathbf{Pr}$ ($\mathbf{Pr} = \nu_1/a_1$, $a_1 = k_1/(\rho_1 c_{p1})$, $\nu_1 = \mu_1/\rho_1$), $\mu_1 = \mu_{10}(T_1/T_{10})^m$. The Prandtl number **Pr** is taken at $T_1 = T_{10}$, and m is some constant, which is different for the different gases [25], [26], e.g. for the steam it is normally in the range: m=0.5–1.0. But it must be noted that such empirical correlations are working only in the narrow temperature intervals by a high gas pressures.

The equation of state [25] has been used in (4): $p_1 = \rho_1 R T_1$, which is used at the temperatures and pressures characteristic of many compressible flow applications. Here R is the specific gas constant, which is a different value for different gases (and steams far from the condensation point). Using this equation of state makes possible, by numerical solution of the full boundary problem for the equation array (1)-(5), to calculate the some parameter, for example, gas density ρ_1^0 twice: from the equation of state and from the mass concervation equation (1) as well. This is good opportunity to control the accuracy of the numerical solution, which was done in the mathematical simulation described further in this paper.

In the equations (5) there are j=2, 3, so that by j=2 it is the energy equation for the solid particles and by j=3 (5) it is the energy equation for the surrounding heat conductive medium. All the values with "0" indexes are taken at the fixed temperature T_{j0}, α is volume fraction of the corresponding phase, c_{v1}, c_{p1} and c_j are specific heat capacity for gas by constant volume and constant pressure, and for solid phases, respectively. Thus the heat conductivity and viscosity of the gas are the same temperature dependent functions.

The terms Q_Σ and Q_V in the equations (4), (5) are specific solid-liquid interfacial heat flux and volumetric heat source, correspondingly. If particles are producing internal heat (e.g. they are electroconductive and current passes through the particles), then the heat sources like Q_V should be excluded from the equation (4) and placed in the equation (5). In general, both of them can have their own heat sources, so that the terms like Q_V are present in both equations. In correspondence with [16], here are:

$$Q_\Sigma = 4\pi b^2\beta_1(T_1 - T_\Sigma), \qquad T_\Sigma = \frac{k_1\mathbf{Nu}_1T_1 + k_2\mathbf{Nu}_2T_2}{k_1\mathbf{Nu}_1 + k_2\mathbf{Nu}_2},$$

where b is the characteristic particle radius, β_1 is the heat exchange coefficient between gas flow and Σ - phase, which is intermediate molecular scale layer between gas and particle with avaraged properties. For the Nusselt number by particles, it was supposed that $\mathbf{Nu}_2 \approx 2$. For the Nusselt number by gas the Frosling law was used: $\mathbf{Nu}_1 = 2 + 0.6\mathbf{Pr}^{1/3}\sqrt{\mathbf{Re}_v}$, where $\mathbf{Re}_v = w_0 b_1/\nu_{10}$ is the Reynolds number by pores in the layer, b_1, w_0, ν_{10} are the characteristic pore radius in the layer, vertical gas filtration velocity and kinematic viscosity by given temperature $T_1 = T_{10}$, respectively.

B. Boundary conditions

System is considered symmetrical relatively to a vertical axis:

$$x = 0, \qquad \partial T_1/\partial x = \partial T_2/\partial x = 0. \quad (6)$$

The normal velocity is zero at the non-permeable boundary, where the continuity of the temperature profiles and heat fluxes must be satisfied:

$$x = x_L, \quad u_1 = 0, \quad T_j = idem, \quad k_2 \partial T_2 / \partial x = k_3 \partial T_3 / \partial x. \qquad (7)$$

It was assumed $k_1 << k_2$, therefore a heat flux from particles to surrounding impermeable medium prevails the one from gas flow. The temperature in surrounding impermeable medium has to be stable far from the boundary of a permeable layer:

$$x = x_\infty, \qquad \partial T_3 / \partial x = 0, \qquad (8)$$

where $x_\infty >> x_L$ is.

The temperatures of a media at the inlet in a particle layer and bottom surface of impermeable medium is known:

$$z = -H, \qquad T_j = T_{jH}, \quad \text{j=1, 2, 3.} \qquad (9)$$

At the outlet of the layer, the heat transfer with surrounding medium is considered. And it is also assumed that the gas pressure is known and temperature gradient at the outlet (the top surface of the layer) is constant. Thus the boundary conditions are:

$$z = 0, \quad p_1 = p_{1H}, \quad \frac{\partial T_1}{\partial z} = const, \quad k_j \frac{\partial T_j}{\partial z} = \beta_j^{top} (T_j - T_{top}), \qquad (10)$$

where T_{top} is the temperature of a surrounding gas medium at the top of the layer, j=2, 3, β_j^{top} is a heat exchange coefficient for particles (j=2) and impermeable medium (j=3).

C. Initial conditions

$$t = 0, \qquad p_1 = p_1^0(x,z), \qquad T_j = T_j^0(x,z), \qquad (11)$$

where is j=1, 2, 3 for the gas, particles and impermeable surrounding medium, respectively. If the gas state equation is used, the initial gas pressure spatial distribution $p_1 = p_1^0(x,z)$ in (11) can be identically replaced by the gas density distribution $\rho_1^0 = \rho_{10}^0(x,z)$.

The initial temperature distribution for the surrounding medium, $T_3 = T_3^0(x,z)$ is normally chosen as uniform, at least by one coordinate, or constant in the whole domain. The surroundings may do the heat release from the saturated particle layer or perform the thermal isolation of the layer. In the last case, the energy equation for the surroundings is omitted and the temperature at the sidewall is kept constant, which simplifies the problem.

IV. SIMPLIFICATION OF THE MODEL

A. Estimation of the parameters in the basic equations

The gas pressure at the inlet in the particle layer supposed to be constant with small fluctuations (e.g. of the same order as the ones caused by temperature fluctuations). Therefore the inertial forces in the equations (2), (3) can be neglected. The vertical pressure gradient is mainly due to the gravity while the horizontal pressure gradient is caused only by the temperature gradient. Thus the vertical gas velocity exceeds the horizontal one a lot. Now the vertical velocity and pressure gradient are calculated from the equations (2), (3) as follows:

$$w_1 = (\rho_1 + \rho_2 - \rho_1^0) \frac{gK}{\mu_1}, \qquad \frac{\partial p_1}{\partial z} = -(\rho_2 + \rho_1) g. \qquad (12)$$

The equations (12) simplify the problem analyzed further in detail. For the accuracy estimation the equation (12) can be even more simplified assuming that $\rho_2 + \rho_1$ is constant. Then the approximate solution yields: $p_1 = -(\rho_2 + \rho_1) gz + p_1^0 + P_1(x)$. Here p_1^0 is constant, $P_1(x)$ is some initial pressure fluctuation by x, which can be zero.

Gas density ρ_1^0 (and, consequently, ρ_1) is small comparing to the particle density ($\rho_1^0 << \rho_2$) but it is kept in the equations (12) because it is spatially and temporary variable and may cause fluctuations of the other parameters in the system. The other peculiarity of the model is that the equations (2), (3) result in the following formula for the horizontal gas velocity

$$u_1 = (1 + 0.5\alpha_2) \frac{K_0 \alpha_2}{\mu_1 \alpha_1} \frac{\partial p_1}{\partial x},$$

which contains the physical contradiction: flow with positive pressure gradient. This may be explained as follows. The heterogeneous model for the gas saturated particle layer [16] was obtained as limit case of the multiphase gas-particle flow when the solid particles become immovable ($\vec{v}_2 = 0$). And our assumption made seems to be too rough as concern to the horizontal gas flow. Namely, it was stated that $\rho_2 \partial u_2 / \partial t << \rho_1 \partial u_1 / \partial t$. But, though it was assumed that $u_2 = 0$, and hence $u_1 >> u_2$ supposed to be, nevertheless $\rho_1 << \rho_2$ is. Therefore the inertial gas flow and "immovable" solid particle forces can be nearly of the same order because the horizontal gas flow is only due to the thermal convection caused by temperature gradient.

B. Darcy law

The following way is proposed to avoid the above-mentioned contradiction. The equation (12) corresponds, with accuracy to the third term in the brackets, to the Darcy's law. Since the horizontal gas flow velocity u_1 is small in comparison with the vertical one ($u_1 << w_1$), the Darcy's law can be also employed: $u_1 = -(K_0 / \mu_1) \partial p_1 / \partial x$.

C. Further simplification of the model

Now let us estimate the second term of the equation (1) comparing to the third and fourth ones. Since $u_1 << w_1$ is, one can analyze only the terms with w_1, except the case of a narrow porous layer, which is not considered here. So that

$u_1 \partial\rho_1^0/\partial x << w_1 \partial\rho_1^0/\partial z$. And, with account of the equation (6), the following estimation yields

$$\frac{w_1 \partial\rho_1^0/\partial z}{\rho_1^0 \partial w_1 \partial z} = \frac{w_1 \partial\rho_1^0}{\rho_1^0 \partial w_1} \propto \frac{\rho_2}{\rho_1} >> 1.$$

Hence the equation (1) is simplified as follows:

$$\frac{\partial\rho_1^0}{\partial t} + \rho_1^0\left(\frac{\partial u_1}{\partial x} + \frac{\partial w_1}{\partial z}\right) = 0. \quad (13)$$

V. Nondimensionalization of the Model

A. Dimensionless equation array

The mathematical model obtained includes the equation array (4), (5), (12), (13) with the initial and boundary conditions (6)-(11). Now for the numerical solution of the boundary problem stated and further analysis of the results, it is more convenient to consider the boundary problem stated in a dimensionless form. For this purpose, the following length, time, velocity, pressure and temperature scales are introduced: H, H^2/a_2^0, a_2^0/H, $\mu_{10}a_2^0/K_0$ and ΔT as the characteristic temperature in a system. Thus the equation array is presented as follows:

$$u_1 = -\frac{\partial p_1}{\partial x}\left(\frac{T_{10}}{T_1}\right)^m, \quad \frac{\partial\rho_1^0}{\partial \mathbf{Fo}} = -\rho_1^0\left(\frac{\partial u_1}{\partial x} + \frac{\partial w_1}{\partial z}\right),$$

$$w_1 = (1-\alpha_1)\left[\mathbf{Pe} - \kappa_\rho \mathbf{Ra}^*(T_2 - T_{20}) - \mathbf{Re}_*^2 \frac{p_1}{T_1}\right]\left(\frac{T_{10}}{T_1}\right)^m,$$

$$\frac{\partial p_1}{\partial z} = \mathbf{Pe}(\alpha_1 - 1)\left[1 - \Delta_2(T_2 - T_{20})\right] - \mathbf{Re}_*^2 \frac{\alpha_1 p_1}{T_1},$$

$$\frac{\partial T_1}{\partial \mathbf{Fo}} = (1-\gamma_1)T_1\left(\frac{\partial u_1}{\partial x} + \frac{\partial w_1}{\partial z}\right) - \left(u_1\frac{\partial T_1}{\partial x} + w_1\frac{\partial T_1}{\partial z}\right) + (\gamma_1 - 1)(u_1^2 +$$

$$+ w_1^2)\left(\frac{T_{10}}{T_1}\right)^m \frac{T_1}{p_1} + \frac{\gamma_1 \mathbf{Pe}(T_1/T_{10})^m}{\alpha_1 \kappa_a \kappa_\rho \mathbf{Re}_*^2 p_1} \bullet$$

$$\bullet\left\{T_1\left(\frac{\partial^2 T_1}{\partial x^2} + \frac{\partial^2 T_1}{\partial z^2}\right) + m\left[\left(\frac{\partial T_1}{\partial x}\right)^2 + \left(\frac{\partial T_1}{\partial z}\right)^2\right] + \xi \mathbf{Nu}_1 T_1(T_2 - T_1)\right\},$$

$$\frac{\partial T_2}{\partial \mathbf{Fo}} = \frac{(1-\alpha_1)^{-1}}{1 - \Delta_2(T_2 - T_{20})}\left[\frac{\partial^2 T_2}{\partial x^2} + \frac{\partial^2 T_2}{\partial z^2} + \xi \frac{\mathbf{Nu}_1}{\kappa_k}\left(\frac{T_1}{T_{10}}\right)^m (T_1 - T_2)\right],$$

$$\frac{\partial T_3}{\partial \mathbf{Fo}} = a_{32}\left(\frac{\partial^2 T_3}{\partial x^2} + \frac{\partial^2 T_3}{\partial z^2}\right). \quad (14)$$

B. The initial and boundary conditions

The initial and boundary conditions (6)-(11) have the following dimensionless form:

$$\mathbf{Fo} = 0, \quad p_1 = p_1^0(x,z), \quad T_j = T_j^0(x,z), \quad \text{j=1, 2, 3;}$$

$$z = 0, \quad p_1 = p_1^{top}, \quad \frac{\partial^2 T_1}{\partial z^2} = 0, \quad \frac{\partial T_j}{\partial z} = N_j^{top}(T_j - T_{top});$$

$$z = -1, \quad T_j = T_{jH}, \quad \text{j=1, 2, 3;} \quad (15)$$

$$x = 0, \quad \frac{\partial T_1}{\partial x} = \frac{\partial T_2}{\partial x} = 0; \quad x = x_\infty, \quad \frac{\partial T_3}{\partial x} = 0;$$

$$x = x_L, \quad u_1 = 0, \quad T_j = idem, \quad \frac{\partial T_2}{\partial x} = k_{32}\frac{\partial T_3}{\partial x}.$$

Here are the following dimensionless criteria: $\mathbf{Pe} = w_0 H/a_2^0$ - Peclet number, $\mathbf{Re}_*^2 = gH/(R\Delta T)$, $\mathbf{Ra}^* = \mathbf{GrPr}^*\mathbf{Da}$ - Rayleigh number, $\mathbf{Gr} = g\Delta_2 H^3 \nu_{10}$, $\mathbf{Pr}^*$ and $\mathbf{Da} = K/H^2$ - Grasshoff, Prandtl and Darcy numbers, respectively, $\mathbf{Fo} = a_2^0 t/H$ - Fourier number. Then $w_0 = \rho_{20}^0 Kg/\mu_{10}$ is the character filtration velocity, a is the heat diffusivity coefficient, e.g. $a_1^0 = k_1^0/(c_{p1}\rho_{10}^0)$. The other parameters are the following: $\kappa_a = a_2^0/a_1^0$, $\kappa_\rho = \rho_{20}^0/\rho_{10}^0$, $\kappa_k = k_2/k_1^0$, $k_{32} = k_3/k_2$, $\gamma_1 = c_{p1}/c_{v1}$, $a_{32} = a_3/a_2^0$, $\xi = s_{12}H^2/b_1$ (parameter of the structure of the granular layer), s_{12} is the specific interfacial area, $b_1 = b\sqrt{2(2-\pi/3)\pi}$ is the character pore radius, b - particle radius (constant in each monolayer), $\Delta_2 = \Delta T\beta_{T2}$, β_{T2} is the particle thermal expansion coefficient.

The system considered is multiphase, an interactions of three different processes occur: non-thermal equilibrium between gas and solid particles in the layer, non-linear processes' mutual influence and non-linearity of the physical properties of gas and particles (mainly, gas properties are strongly dependent on the temperature pressure). The first above-mentioned peculiarity is touched with the term $\xi(T_1 - T_2)$, which describes the local heat transfer between particles and flow.

From the mathematical point of view it causes some limitation on the parameter ξ because the term $\xi(T_1 - T_2)$ in the energy equations for solid particles and gas flow appears to be huge by very small particles. And these energy equations have terms like "$\infty \bullet 0$" because by small particles the temperature difference $(T_1 - T_2)$ is going fast to zero. Therefore as far as the temperature difference between particles and gas flow is going to zero, in limit there is the homogeneous mixture. Then heterogeneous model considered should be replaced with a homogeneous one to avoid this peculiarity causing numerical inaccuracy.

The most important new phenomenon is a localization of the dissipate processes due to non-linear heat conductivity. This phenomenon was studied at first by Samarskii et. al. [27] for quasilinear parabolic equations, e.g. one-dimensional heat conductivity equation with a non-linear heat conductivity $k = k_0 T^m$ (m=0.5–1.0). Some gases and steam follow this law under certain range of the temperature and pressure. In our case all these phenomena are interconnected.

VI. Numerical Solution of the Boundary Problem

A. Numerical algorithm

For the numerical solution of the boundary problem (14), (15), the method of fractional steps (MFS) developed by Janenko

[28] was employed as effective and simple one. The strategy of the method is in a split of a basic equation into several equations each of those is one-dimensional equation. The basics of this method can be explained on the example of a two-dimensional diffusion equation.

The numerical scheme considered below could be generalized from two to three spatial variables, therefore a two-dimensional equation is considered just for simplicity:

$$\frac{\partial \overline{T}}{\partial t}-\alpha_x\frac{\partial^2 \overline{T}}{\partial x^2}-\alpha_y\frac{\partial^2 \overline{T}}{\partial y^2}=0.$$

By the method of fractional steps, instead of this equation, the following equation array is introduced:

$$0.5\frac{\partial \overline{T}}{\partial t}-\alpha_y\frac{\partial^2 \overline{T}}{\partial y^2}=0,\qquad 0.5\frac{\partial \overline{T}}{\partial t}-\alpha_x\frac{\partial^2 \overline{T}}{\partial x^2}=0,$$

so that the full approximation is achieved at a whole time-step.

Each equation is discreted and solved consequently by each time step using the well-known one-dimensional numerical schemes. The implicit method of fractional steps (MFS) when applied for the equation array using Crank-Nicolson scheme yields in the following approximation

$$\left(1-0.5\alpha_y\Delta t L_{yy}\right)T_{j,k}^{n+1/2}=\left(1+0.5\alpha_y\Delta t L_{yy}\right)T_{j,k}^{n},$$
$$\left(1-0.5\alpha_x\Delta t L_{xx}\right)T_{j,k}^{n+1}=\left(1+0.5\alpha_x\Delta t L_{xx}\right)T_{j,k}^{n+1/2}.$$

The system results in an algebraic equation array with a block tridiagonal matrix along the numerical grid lines. Thus the solution at each half-step is found using the Thomas's marching algorithm [29]. This scheme has an accuracy order of $\approx O\left((\Delta t)^2,(\Delta x)^2,(\Delta y)^2\right)$ and is absolutely stable by the proper boundary conditions both for the two-dimensional as well as for the three-dimensional cases.

B. Split procedure

Numerical solution of the boundary problem (14), (15) has been performed using the method of fractional steps. Splitting between the spatial variables transformed the two-dimensional problem to the two separated one-dimensional problems. *On the lower half-step (the first temporal semi-step):*

$$\frac{\partial p_1}{\partial z}=\mathbf{Pe}(\alpha_1-1)\left[1-\Delta_2(T_2-T_{20})\right]-\mathbf{Re}_*^2\frac{\alpha_1 p_1}{T_1},$$
$$\frac{1}{2}\frac{\partial T_3}{\partial \mathbf{Fo}}=a_{32}\frac{\partial^2 T_3}{\partial x^2},\qquad \frac{1}{2}\frac{\partial \rho_1^0}{\partial \mathbf{Fo}}=-\rho_1^0\frac{\partial u_1}{\partial x},\qquad u_1=-\frac{\partial p_1}{\partial x}\left(\frac{T_{10}}{T_1}\right)^m,$$
$$w_1=(1-\alpha_1)\left[\mathbf{Pe}-\kappa_\rho\mathbf{Ra}^*(T_2-T_{20})-\mathbf{Re}_*^2\frac{p_1}{T_1}\right]\left(\frac{T_{10}}{T_1}\right)^m,$$
$$\frac{1}{2}\frac{\partial T_1}{\partial \mathbf{Fo}}=(1-\gamma_1)T_1\frac{\partial u_1}{\partial x}-u_1\frac{\partial T_1}{\partial x}+(\gamma_1-1)u_1^2\left(\frac{T_{10}}{T_1}\right)^m\frac{T_1}{p_1}+$$
$$+\frac{\gamma_1\mathbf{Pe}\left(T_1/T_{10}\right)^m}{\alpha_1\kappa_a\kappa_\rho\mathbf{Re}_*^2 p_1}\left[T_1\frac{\partial^2 T_1}{\partial x^2}+m\left(\frac{\partial T_1}{\partial x}\right)^2+\alpha\xi\mathbf{Nu}_1T_1(T_2-T_1)\right],\qquad (16)$$
$$\frac{1}{2}\frac{\partial T_2}{\partial \mathbf{Fo}}=\frac{(1-\alpha_1)^{-1}}{1-\Delta_2(T_2-T_{20})}\left[\frac{\partial^2 T_2}{\partial x^2}+\alpha\xi\frac{\mathbf{Nu}_1}{\kappa_k}\left(\frac{T_1}{T_{10}}\right)^m(T_1-T_2)\right].$$

On the upper half-step (the second temporal semi-step):

$$\frac{\partial p_1}{\partial z}=\mathbf{Pe}(\alpha_1-1)\left[1-\Delta_2(T_2-T_{20})\right]-\mathbf{Re}_*^2\frac{\alpha_1 p_1}{T_1},$$
$$\frac{1}{2}\frac{\partial \rho_1^0}{\partial \mathbf{Fo}}=-\rho_1^0\frac{\partial w_1}{\partial z},\qquad u_1=-\frac{\partial p_1}{\partial x}\left(\frac{T_{10}}{T_1}\right)^m,\qquad \frac{1}{2}\frac{\partial T_3}{\partial \mathbf{Fo}}=a_{32}\frac{\partial^2 T_3}{\partial z^2},$$
$$w_1=(1-\alpha_1)\left[\mathbf{Pe}-\kappa_\rho\mathbf{Ra}^*(T_2-T_{20})-\mathbf{Re}_*^2\frac{p_1}{T_1}\right]\left(\frac{T_{10}}{T_1}\right)^m,\qquad (17)$$
$$\frac{1}{2}\frac{\partial T_1}{\partial \mathbf{Fo}}=(1-\gamma_1)T_1\frac{\partial w_1}{\partial z}-w_1\frac{\partial T_1}{\partial z}+(\gamma_1-1)w_1^2\left(\frac{T_{10}}{T_1}\right)^m\frac{T_1}{p_1}+$$
$$+\frac{\gamma_1\mathbf{Pe}\left(T_1/T_{10}\right)^m}{\alpha_1\kappa_a\kappa_\rho\mathbf{Re}_*^2 p_1}\left[T_1\frac{\partial^2 T_1}{\partial z^2}+m\left(\frac{\partial T_1}{\partial z}\right)^2+(1-\alpha)\xi\mathbf{Nu}_1T_1(T_2-T_1)\right],$$
$$\frac{1}{2}\frac{\partial T_2}{\partial \mathbf{Fo}}=\frac{(1-\alpha_1)^{-1}}{1-\Delta_2(T_2-T_{20})}\left[\frac{\partial^2 T_2}{\partial z^2}+(1-\alpha)\xi\frac{\mathbf{Nu}_1}{\kappa_k}\left(\frac{T_1}{T_{10}}\right)^m(T_1-T_2)\right].$$

where $\alpha\in[0;1]$ is the scheme approximation parameter. By choosing this parameter between 0 and 1 the term with phase heat exchange has different influence in first and second half-step. It allows controlling the properties of numerical scheme.

C. Finite-difference approximation of derivatives

Derivatives inside two-dimensional numerical domain are approximated by the second-order central differences:

$$\frac{\partial f}{\partial x}=\frac{f_n^{i+1,j}-f_n^{i-1,j}}{2\Delta x},\qquad \frac{\partial^2 f}{\partial x^2}=\frac{f_n^{i+1,j}-2f_n^{i,j}+f_n^{i-1,j}}{(\Delta x)^2}.$$

At the boundary of domain a 3-point approximation is applied:

$$\frac{\partial f}{\partial x}=\frac{f_n^{3,j}-2f_n^{2,j}+f_n^{1,j}}{2\Delta x}.$$

With regards to a coordinate z approximation of the derivatives are performed similarly.

The temporal derivatives are approximated at each point (i,j) of a numerical domain by first-order forward differences:

$$\frac{\partial f}{\partial \mathbf{Fo}}=\frac{f_{n+1}^{i,j}-f_n^{i,j}}{\Delta\tau},$$

where $\Delta\tau$ is a time step on the numerical grid chosen.

Thus the boundary problem (15)-(17) should be solved numerically. The boundary conditions (15) are splitted for the equation arrays (16) and (17) by x and z, correspondingly.

D. Finite-difference scheme for the boundary problem

The finite-difference scheme for the numerical solution of the boundary problem (15)-(17) with account of the above-mentioned consists of two steps. On the first half-step by time the boundary problem (15), (16) is solved in the following finite-difference form:

$$(\rho_{1,n+0.5}^0)^{i,j}=(\rho_{1,n}^0)^{i,j}+(\rho_{1,n}^0)^{i,j}\frac{\tau}{2h_x}\left[\beta_1(u_{1,n+0.5}^{i-1,j}-u_{1,n+0.5}^{i+1,j})+(1-\beta_1)(u_{1,n}^{i-1,j}-u_{1,n}^{i+1,j})\right],$$
$$p_{1,n}^{i,j+1}=p_{1,n}^{i,j-1}+2h_z\left\{\mathbf{Pe}(\alpha_1-1)\left[1+\Delta_2(T_{20}-T_{2,n}^{i,j})\right]-\alpha_1\mathbf{Re}_*^2\frac{p_{1,n}^{i,j}}{T_{1,n}^{i,j}}\right\},$$
$$u_{1,n}^{i,j}=\frac{p_{1,n}^{i-1,j}-p_{1,n}^{i+1,j}}{2h_x}\left(\frac{T_{10}}{T_{1,n}^{i,j}}\right)^m,\qquad (18)$$

$$w_{1,n}^{i,j}=(1-\alpha_1)\left\{\mathbf{Pe}\left[1+\Delta_2(T_{20}-T_{2,n}^{i,j})\right]-\mathbf{Re}_*^2\frac{p_{1,n}^{i,j}}{T_{1,n}^{i,j}}\right\}\left(\frac{T_{10}}{T_{1,n}^{i,j}}\right)^m,$$

$$\frac{T_{1,n+0.5}^{i,j}-T_{1,n}^{i,j}}{\tau}=\frac{1-\gamma_1}{2h_x}\left[\beta T_{1,n+0.5}^{i,j}+(1-\beta)T_{1,n}^{i,j}\right]\left[\beta_1(u_{1,n+0.5}^{i+1,j}-u_{1,n+0.5}^{i-1,j})+(1-\beta_1)(u_{1,n}^{i+1,j}-u_{1,n}^{i-1,j})\right]+$$

$$+\frac{1}{2h_x}\left[(\beta_1-1)u_{1,n}^{i,j}-\beta_1 u_{1,n+o.5}^{i,j}\right]\left[\beta(T_{1,n+0.5}^{i+1,j}-T_{1,n+0.5}^{i-1,j})+(1-\beta)(T_{1,n}^{i+1,j}-T_{1,n}^{i-1,j})\right]+$$

$$+(\gamma_1-1)\left[\beta_1(u_{1,n+0.5}^{i,j})^2+(1-\beta_1)(u_{1,n}^{i,j})^2\right]\frac{\left[\beta T_{1,n+0.5}^{i,j}+(1-\beta)T_{1,n}^{i,j}\right]^{m+1}}{\left[\beta_2 p_{1,n+0.5}^{i,j}+(1-\beta_2)p_{1,n}^{i,j}\right]T_{10}^m}+$$

$$+\frac{\gamma_1\mathbf{Pe}\left[\beta T_{1,n+0.5}^{i,j}+(1-\beta)T_{1,n}^{i,j}\right]^m}{\alpha_1\kappa_a\kappa_\rho\mathbf{Re}_*^2\left[\beta_2 p_{1,n+0.5}^{i,j}+(1-\beta_2)p_{1,n}^{i,j}\right]T_{10}^m}\left\{\left[\beta_2 T_{1,n+0.5}^{i,j}+(1-\beta_2)T_{1,n}^{i,j}\right]\left[\beta(T_{1,n+0.5}^{i+1,j}-2T_{1,n+0.5}^{i,j}+\right.\right.$$

$$\left.\left.+T_{1,n+0.5}^{i-1,j})+(1-\beta)(T_{1,n}^{i+1,j}-2T_{1,n}^{i,j}+T_{1,n}^{i-1,j})\right]\frac{1}{h_x^2}+\frac{m}{4h_x^2}\left[\beta_2(T_{1,n+0.5}^{i+1,j}-T_{1,n+0.5}^{i-1,j})+(1-\beta_2)(T_{1,n}^{i+1,j}-T_{1,n}^{i-1,j})\right]^2+\right.$$

$$\left.+\alpha_2\mathbf{Nu}_1\left[\beta_2 T_{1,n+0.5}^{i,j}+(1-\beta_2)T_{1,n}^{i,j}\right]\left[\beta_5 T_{2,n+0.5}^{i,j}+(1-\beta_5)T_{2,n}^{i,j}-\beta_5 T_{1,n+0.5}^{i,j}+(\beta_5-1)T_{1,n}^{i,j}\right]\right\},$$

$$\frac{T_{2,n+0.5}^{i,j}-T_{2,n}^{i,j}}{\tau}(1-\alpha_1)\left\{1+\Delta_2\left[T_{20}-\beta_4 T_{2,n+0.5}^{i,j}+(\beta_4-1)T_{2,n}^{i,j}\right]\right\}=\frac{1}{h_x^2}\left[\beta(T_{2,n+0.5}^{i+1,j}-2T_{2,n+0.5}^{i,j}+\right.$$

$$\left.+T_{2,n+0.5}^{i-1,j})+(1-\beta)(T_{2,n}^{i+1,j}-2T_{2,n}^{i,j}+T_{2,n}^{i-1,j})\right]+\frac{\alpha_2\mathbf{Nu}_1}{\kappa_k T_{10}^m}\left[\beta_3 T_{1,n+0.5}^{i,j}+(1-\beta_3)T_{1,n+0.5}^{i,j}\right]^m\cdot$$

$$\cdot\left[\beta_5(T_{1,n+0.5}^{i,j}-T_{2,n+0.5}^{i,j})+(1-\beta_5)(T_{1,n}^{i,j}-T_{2,n}^{i,j})\right],$$

$$\frac{T_{3,n+0.5}^{i,j}-T_{3,n}^{i,j}}{\tau}=\frac{a_{32}}{h_x^2}\left[\beta(T_{3,n+0.5}^{i+1,j}-2T_{3,n+0.5}^{i,j}+T_{3,n+0.5}^{i-1,j})+(1-\beta)(T_{3,n}^{i+1,j}-2T_{3,n}^{i,j}+T_{3,n}^{i-1,j})\right],$$

where τ, h_x and h_z are the steps by time (Fourier number) and two spatial variables x, z, respectively. And the indeces n, *i, j* are used with respect to the corresponding numerical grid points for all above-mentioned variables. The first bottom index has been retained the same as previously for all variables. The second bottom index is temporal grid point (n). The top indeces are the spatial numerical grid points by *x (i)* and *z (j),* respectively.

Then the finite-difference equation array on the upper temporal semi-step may be got similarly to (18). Here the constants β, β_j (j=1-5) are weighting coefficients of the numerical scheme like the above-mentioned α. They are introduced for the controlling possibility in numerical scheme.

E. The finite-difference boundary and initial conditions

Initial and boundary conditions (15) in a finite-difference representation yield

$$\begin{aligned}
&p_{1,1}=p_1^0(i,j),\quad T_{1,1}=T_1^0(i,j),\quad T_{2,1}=T_2^0(i,j),\quad T_{3,1}=T_3^0(i,j);\\
&p_{1,n}^{i,1}=p_1^{top}(i),\quad T_{1,n}^{i,1}=\frac{1}{3}(4T_{1,n}^{i,2}-T_{1,n}^{i,3}),\quad T_{3,n}^{I,j}=\frac{1}{3}(4T_{3,n}^{I-1,j}-T_{3,n}^{I-2,j});\\
&T_{l,n}^{i,1}=\frac{T_{l,n}^{i,3}-4T_{l,n}^{i,2}+2h_z N_l^{top}T_{top}}{2h_z N_l^{top}-3},\quad l=2,3;\\
&T_{1,n}^{i,J}=T_{1H}(i),\qquad T_{2,n}^{i,J}=T_{2H}(i),\qquad T_{3,n}^{i,J}=T_{3H}(i);\\
&T_{1,n}^{1,j}=\frac{1}{3}(4T_{1,n}^{2,j}-T_{1,n}^{3,j}),\qquad T_{2,n}^{1,j}=\frac{1}{3}(4T_{2,n}^{2,j}-T_{2,n}^{3,j});
\end{aligned}\tag{19}$$

$$\begin{aligned}
&u_{1,n}^{I,j}=0,\qquad T_{1,n}^{I,j}=T_{2,n}^{I,j}=T_{3,n}^{I,j},\\
&3T_{2,n}^{I,j}-4T_{2,n}^{I-1,j}+T_{2,n}^{I-2,j}=k_{32}(3T_{3,n}^{1,j}-4T_{3,n}^{2,j}+T_{3,n}^{3,j});\qquad .
\end{aligned}$$

Here are: $i=\in[1,I]$, $j\in[1,J]$ so that the numerical grid contains I nodes by x in the particle layer and in the impermeable surrounding medium, which are numbered from the left to the right, and J nodes by z numbered from the top to the bottom.

F. The Thomas' marching procedure

The finite-difference boundary problem (19), (19) was solved numerically using the Thomas' marching procedure [29]. Two three-point scalar marching were applied by x and z. The non-linear terms were computed iteratively: first by the parameters of the previus temporary layer and then the values from the previous iteration were used. The iterations were performed before the two consequent iterations differed less than the control level stated.

The three-point finite-difference boundary problem has been solved on the lower half-step by time using the equations:

$$\begin{aligned}
&T_{l,n+0.5}^{i,j}=A_{l,n+0.5}^{i+1,j}T_{l,n+0.5}^{i+1,j}+B_{l,n+0.5}^{i+1,j},\qquad l=1,2,\\
&T_{3,n+0.5}^{i+1,j}=A_{3,n+0.5}^{i+1,j}T_{3,n+0.5}^{i,j}+B_{3,n+0.5}^{i+1,j}.
\end{aligned}\tag{20}$$

On the upper half-step the following equations were used:

$$T_{l,n+1}^{i,j}=C_{l,n+0.5}^{i,j+1}T_{l,n+1}^{i,j+1}+D_{l,n+1}^{i,j+1},\qquad l=1,2,3.\tag{21}$$

The finite-difference equations on the lower half-step yield in a three-diagonal form:

$$E_{l,n+0.5}^{i,j}T_{l,n+0.5}^{i-1,j}-\Gamma_{l,n+0.5}^{i,j}T_{l,n+0.5}^{i,j}+G_{l,n+0.5}^{i,j}T_{l,n+0.5}^{i+1,j}=-F_{l,n+0.5}^{i,j},\tag{22}$$

where are: $i\in[2,I-1]$, $l=1,2,3$ (for gas, particles and impermeable medium, respectively). The coefficients E,Γ,G,F are cumbersome, therefore they are omitted. Similarly on the upper half-step:

$$E_{l,n+1}^{i,j}T_{l,n+1}^{i,j-1}-\Gamma_{l,n+1}^{i,j}T_{l,n+1}^{i,j}+G_{l,n+1}^{i,j}T_{l,n+1}^{i,j+1}=-F_{l,n+1}^{i,j},\tag{23}$$

where are: $j\in[2,J-1]$, $l=1,2,3$.

The equations (20), (21) with the boundary and initial conditions (19) give the following marching coefficients:

$$\begin{aligned}
&A_{l,n+0.5}^{i+1,j}=\frac{G_{l,n+0.5}^{i,j}}{\Gamma_{l,n+0.5}^{i,j}-E_{l,n+0.5}^{i,j}A_{l,n+0.5}^{i,j}},\quad A_{3,n+0.5}^{i,j}=\frac{E_{3,n+0.5}^{i,j}}{\Gamma_{3,n+0.5}^{i,j}-G_{3,n+0.5}^{i,j}A_{3,n+0.5}^{i+1,j}},\\
&B_{l,n+0.5}^{i+1,j}=\frac{E_{l,n+0.5}^{i,j}B_{l,n+0.5}^{i,j}+F_{l,n+0.5}^{i,j}}{\Gamma_{l,n+0.5}^{i,j}-E_{l,n+0.5}^{i,j}A_{l,n+0.5}^{i,j}},\quad B_{3,n+0.5}^{i+1,j}=\frac{G_{3,n+0.5}^{i,j}B_{3,n+0.5}^{i+1,j}+F_{3,n+0.5}^{i,j}}{\Gamma_{3,n+0.5}^{i,j}-G_{3,n+0.5}^{i,j}A_{3,n+0.5}^{i+1,j}},
\end{aligned}\tag{24}$$

where the boundary values of the coefficients calculated by the boundary conditions are:

$$A^{2,j}_{l,n+0.5}=1,\quad B^{2,j}_{l,n+0.5}=0,\quad l=1,2;\quad A^{I,j}_{3,n+0.5}=1,\quad B^{I,j}_{3,n+0.5}=0;$$

$$T^{I,j}_{l,n+0.5}\equiv T^{I,j}_{n+0.5}=\frac{k_{23}B^{I,j}_{2,n+0.5}+B^{2,j}_{3,n+0.5}}{1-A^{2,j}_{3,n+0.5}+k_{23}\left(1-A^{I,j}_{2,n+0.5}\right)},\quad l=1,2,3. \qquad (25)$$

The marching is going to the right with $l=1,2$ and to the left with $l=3$.

On the upper temporal half-step all the marching is right:

$$C^{i,j+1}_{l,n+1}=\frac{G^{i,j}_{l,n+1}}{\Gamma^{i,j}_{l,n+1}-E^{i,j}_{l,n+1}C^{i,j}_{l,n+1}},\quad D^{i,j+1}_{l,n+1}=\frac{E^{i,j}_{l,n+1}D^{i,j}_{l,n+1}+F^{i,j}_{l,n+1}}{\Gamma^{i,j}_{l,n+1}-E^{i,j}_{l,n+1}C^{i,j}_{l,n+1}}, \qquad (26)$$

where are:

$$D^{i,2}_{l,n+1}=\frac{h_z N^{top}_l T_{top}}{h_z N^{top}_l-1},\quad T^{i,J}_{l,n+1}=\frac{\Theta_{k,n+1}-D^{i,J}_{l,n+1}}{A^{i,J}_{l,n+1}-1},\quad C^{i,2}_{1,n+1}=1,$$

$$C^{i,2}_{l,n+1}=\frac{1}{h_z-N^{top}_l},\ D^{i,2}_{1,n+1}=0,\quad \Theta_{k,n+1}=T^{i,J}_{l,n+1}-T^{i,J-1}_{l,n+1}\ . \qquad (27)$$

The relations (24)-(27) finalize the numerical solution.

VII. COMPUTER SIMULATION OF THE GEOTHERMAL SYSTEM

A. Parameters of the geothermal system

The model obtained was implemented for numerical simulation by the following parameters for steam flow through the geothermal underground layer:

K_0=1.5*10^{-14}m^2, H =10^{3}m, ΔT =200K, ρ^0_{10}=0.58kg/m^3, ρ^0_{20}=2.6*10^{3}kg/m^3, a^0_1=2.04*10^{-5}m^2/s, a^0_2=6.3*10^{-7}m^2/s, k^0_1=24.1*10^{-3}W/(m*K), k^0_2=1.58W/(m*K), β_{T2}=10^{-5}K^{-1}, γ_1=1.28, μ_{10}=1.24*10^{-5}N*s/m^2, α_1=0.26, T_{10}=1.865, p_{1H} =1.52*10^{5}N/m^2, $\mathbf{Re}^2_*$=0.113, **Pe** =5*10^4, **Da** =1.5*10^{-20}, **Pr** =1.05*10^{-3}, $\mathbf{Ra}^*$=47.7, $\mathbf{Nu}_1$=2.01, **Gr** =9.35*10^{22}, $T^0_j(x,z)=T^0_{j0}-c_j z$, where c_j=const.

B. Results of computer simulations for geothermal system

The results of computations are presented in Figs 2, 3:

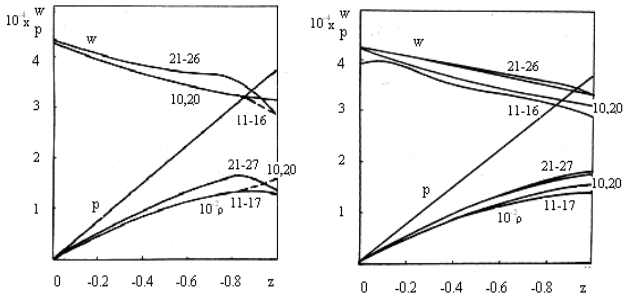

Fig. 2. Vertical velocity, pressure and density of steam on the grids 11x6 (to the left) and 21x11 (to the right)

The grid 11x6 is too robust but 21x11 gives attainable results of computations, so that more fine grids are not needed in a majority of computations. Fig. 2 shows the difference between the numerical solutions on those two grids applied. Computations on the grids 41x21 did not show remarkable difference with 21x11.

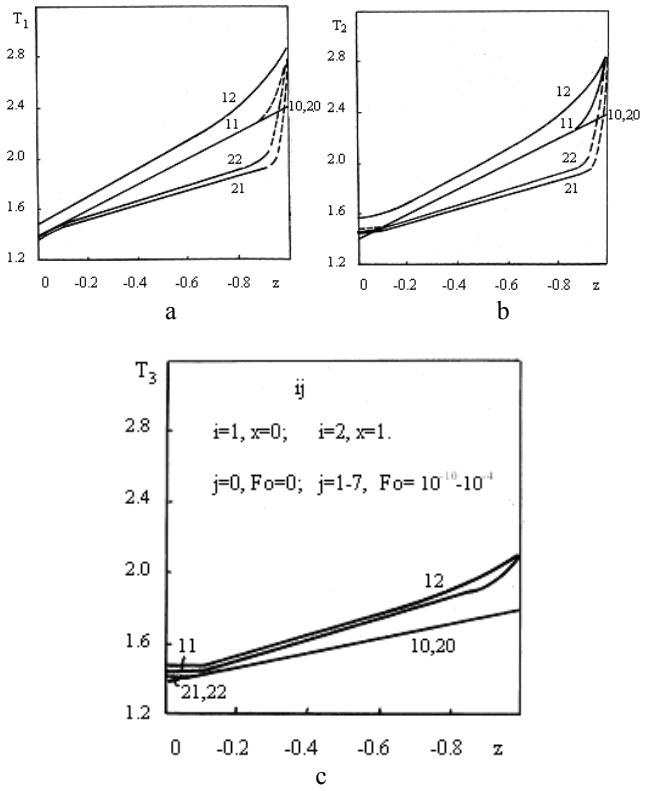

Fig. 3. Steam temperature (a), particles temperatures (b) and temperature of the surroundings (c) on the grid 21x11

The numerical simulations show that two consecutive temporal iterations at each temporal step completely coincide with accuracy up to five digits if time step is below 10^{-8}. In the case considered Fourier number (dimensionless time) Fo=10^{-5} corresponds to approximately one year. Only horizontal steam flow velocity may differ but it is too small comparing to the vertical one (no more than 1%, mainly 4-6 order less than vertical depending on permeability of particle layer).

The difference in results of computations on the numerical grids 11x6 and 21x11 reveal remarkable only near the upper and bottom boundaries of the layer being mainly neglegible inside the layer (less than 5%). The computations with using the grids 21x11 and 41x21 are practically coinciding.

Data presented in Figs 2, 3 show that the system studied is inertial so that the non-stationary effects reveal approximately starting from Fo=10^{-7}. The maximal temperature difference between the particles and steam is observed near the upper and bottom boundaries of the layer, while inside the layer all parameters are close to some linear functions of vertical coordinate z.

With the stated here initial temperature distributions, which depend only on z, the numerical simulation has showed no remarkable changes of parameters by coordinate x with further evolution of the system in time, except narrow region close to the interfacial boundary between particle layer and impermeable medium. In these narrow regions the flow

velocity exceeds the one in the rest of numerical domain about 5-15% with increase near the bottom boundary z=-1. A variation of the steam density is the most intensive (0-30%), and influence of particle layer on the impermeable medium is negligible. Its temperature is varying only near the interfacial boundary rapidly decreasing far from boundary, so that in many applications it may be neglected. Thus, only a heat flux from particle layer into the impermeable medium must be taken into account in boundary conditions omitting the heat conductivity equation for surroundings. This simplification of the problem can be made in all situations when impermeable medium has substantial thermal resistance working as insulator for the particle layer. If impermeable medium serves for the heat removal (its thermal conductivity is higher than thermal conductivity of particle layer), then the above-mentioned model is appropriate for numerical simulation.

C. Perturbation of the system

Now let us consider more complex case when the initial state of the system in substantially non-uniform as it is normally observed in engineering practice. For example, the initial temperature of steam is perturbed [1, 4]:

$$T_1^0 = T_{10}^0(x,z) + \theta_1 \sin k_1 x \sin m_1 z, \quad (28)$$

$T_{10}^0(x,z)$ is an initial unperturbed temperature distribution, θ_1 is amplitude of perturbation, and k_1, m_1 are the wave numbers of perturbations by x and z, respectively.

D. Blow-up regimes

The results of computer simulation for porosity $\alpha_1 = 0.26$, $\xi = 4 \cdot 10^4$ (particles of the layer are nearly 1m in diameter for the layer of H=10^3 m) are given in Figs. 4-6:

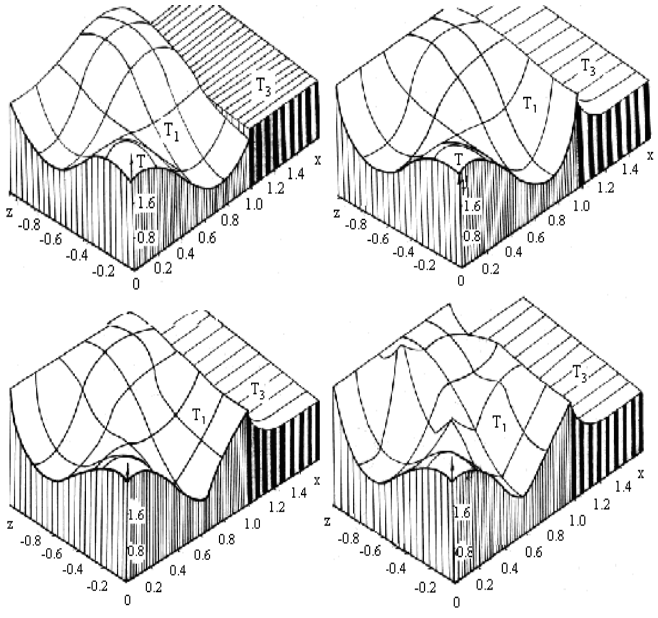

Fig. 4. Temperature evolution in steam flow T_1 and surrounding T_3 for $Fo = 0$, $Fo = 2 \cdot 10^{-7}$, $Fo = 2 \cdot 10^{-6}$ and $Fo = 2 \cdot 10^{-5}$, respectively, computed by $\Delta Fo = 2 \cdot 10^{-8}$.

Fig. 4 shows temperature evolution in a domain. Temperature distribution for particles in the permeable particle layer does not change so much as the temperature of a steam, therefore it is not shown in figure. Then the related evolution of a steam density and its vertical flow velocity is presented in Figs 5, 6:

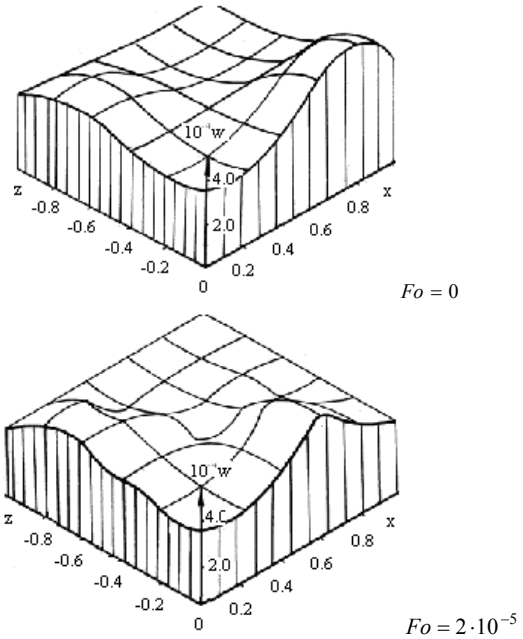

Fig. 5. Evolution of a steam flow velocity in particle layer

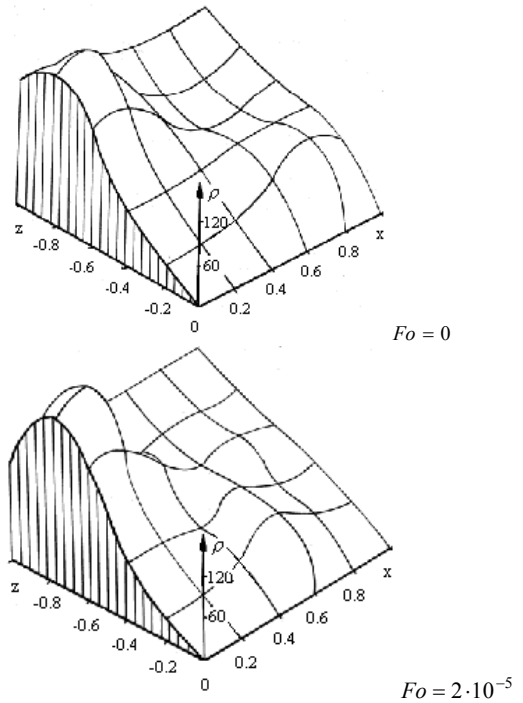

Fig. 6. Evolution of a steam density in particle layer

The non-linear interaction of the perturbations in a system may cause strongly non-uniform evolution of the parameters in the domain. The other case of simulation performed for the same physical situation but with the ten times larger particles in the layer ($\xi = 4 \cdot 10^2$) is presented in Fig. 7 for $Fo = 2 \cdot 10^{-5}$, where from follows that with increase of particle size the heterogeneous properties and localization of abnormal heating reveal more definitely:

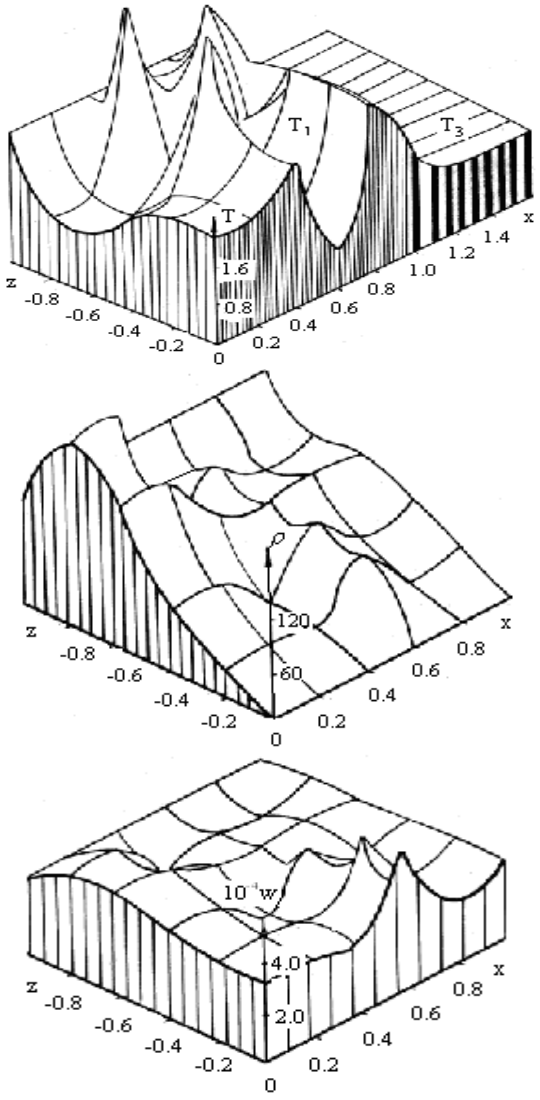

Fig. 7. Local abnormal heating in particle layer and non-linear interaction of parameters

VIII. Conclusion

With a local abnormal heating due to non-linear heat conductivity of steam temperature escalation in some narrow regions causes local vicosity increase, which, in turn, leads to decrease in steam flow velocity. Therefore heat conductivity becomes higher while convective heat transfer falls down. Inversely, in the local regions with lower temperature viscosity is lower, thus, velocity of steam flow grows and convective heat transfer dominates, so that in such localities temperature is lower. Local abnormal heating due to non-linear conductivity and non-linear interaction of parameters results in complex non-uniform distribution of the parameters of steam flow in particle layer.

References

[1] I.V. Kazachkov and M.J. Konovalikhin, "Steam Flow Through the Volumetrically Heated Particle Bed", Int. J. of Thermal Sciences, Vol. 41, No. 8, 2002.

[2] M.J. Konovalikhin, Z.L. Yang, M. Amjad and B.R. Sehgal, "On Dryout Heat Flux of a Particle Debris Bed with a Downcomer", ICONE-8, Baltimore, USA, April, 2000.

[3] J. Bear, "Dynamics of fluids in porous media": New York, 1972.

[4] I.V. Kazachkov, "On the Mathematical Simulation of Processes of Non-stationary Non-isothermal Filtration in Geothermal Systems", J. Numer. And Appl. Mathematics, Vol. 60, Kiev University, 1986.

[5] V.M. Polyaev, V.A. Maiorov, L.L. Vasiliev, "Hydrodynamic and Heat Transfer in the Porous Elements of the Avionic Components": Moscow, Mashinostroenie, 1988.

[6] L.I. Heifets, A.V. Neimark, "Multiphase Processes in Porous Media": Moscow, Khimiya, 1982.

[7] M.V. Choudhary and N.M. El-Wakil, "Heat Transfer and Flow Characteristics in Conductive Porous Media with Energy Generation", Proc. Int. Heat Transfer Conf., Versailes, France, 1970.

[8] L.L. Vasiliev and V.A. Mairov, "An Analytical Study of Resistance, Heat Transfer and Stability in Evaporative Cooling of a Porous Heat Producting Element", Int. J. Heat Mass Transfer, 12, 301-307, 1979.

[9] A.S. Naik and V.K. Dhir, "Forced Flow Evaporative Cooling of a Volumetrically Heated Porous Layer", Int. J. Heat Mass Transfer, Vol. 25, No. 4, pp. 541-552, 1982.

[10] G. Hofmann, "On the Location and Mechanisms of Dryout in Top-Fed and Bottom-Fed Particulate Beds", Nuclear Technology, Vol. 65, 1984.

[11] T. Schulenberg and U. Mueller, "A Refined Model for the Coolability of Core Debris with Flow Entry from the Bottom", Presented at the 6th Information Exchange Meeting on Debris Coolability, Univ. of California, Los-Angeles, 1984.

[12] F.P. Tsai, "Dryout heat flux in a volumetrically heated porous bed", Ph.D. Dissertation, Univ. of California, Los Angeles, 1987.

[13] V.X. Tung and V.K. Dhir, "A Hydrodynamic Model for Two-Phase Flow Through Porous Media", Int. J. Multiphase Flow, Vol. 14, No. 1, pp. 47-65, 1988.

[14] V.X. Tung and V.K. Dhir, "Finite Element Solution of Multi-Dimensional Two-Phase Flow Through Porous Media with Arbitrary Heating Conditions", Int. J. Multiphase Flow, Vol. 16, No. 6, pp. 985-1002, 1990.

[15] A.K. Stubos and J.-M. Buchlin, "Analysis and Numerical Simulation of the Thermohydraulic Behavior of a Heat Dissipating Debris Bed During Power Transients", Int. J. Heat Mass Transfer, Vol. 36, No. 5, pp. 1391-1401, 1993.

[16] R.I. Nigmatulin,"The Base of Mechanics of Heterogeneous Media": Moscow, Nauka, 1978.

[17] M. Sözen and K. Vafai, "Analysis of the Non-Thermal Equilibrium Condensing Flow of a Gas Through a Packed Bed", Int. J. Heat Mass Transfer, Vol. 33, No. 6, pp. 1247-1261, 1990.

[18] A.V. Kuznetsov, "An Investigation of a Wave of Temperature Difference Between Solid and Fluid Phases in a Porous Packed Bed", Int. J. Heat Mass Transfer, Vol. 37, No. 18, pp. 3030-3033, 1994.

[19] A.V. Kuznetsov, "Investigation of Multi-Dimensional Effects During Heating a Porous Packed Bed". 2nd European Thermal-Sciences and 14th UIT National Heat Transfer Conference, 1996.

[20] A.V. Kuznetsov, "Thermal Nonequilibrium Forced Convection in Porous Media", Chapter in "{em TransportPhenomena in Porous Media}", D.B. Ingham and I. Pop (Editors), Elsevier, Oxford, 1998, pp. 103-129.

[21] Kazachkov I.V., Konovalikhin M.J. and Sehgal B.R. *Dryout Location in a Low-porosity Volumetrically Heated Particle Bed//* J. of Enhanced Heat Transfer. 2001.- Vol.8, no.6, p.397-410.
[22] B.R. Sehgal, M.J. Konovalikhin, Z.L. Yang, I.V. Kazachkov, M. Amjad, G.J.Li, Investigations on porous media coolability, KTH report, 2001.
[23] Kazachkov I.V. Konovalikhin M.J. and Sehgal B.R. *Coolability of melt pools and debris beds with bottom injection//* 2nd Japanese-European Two-Phase Flow Group Meeting, Tsukuba, Japan, 2000.
[24] Konovalikhin M.J., Kazachkov I.V. and Sehgal B.R. *A model of the steam flow through the volumetrically heated saturated particle bed*/ ICMF 2001: Fourth International Conference on Multiphase Flow, New Orleans, Louisiana, U.S.A., May 27 - June 1, 2001.
[25] F.P. Incropera, D.P. DeWitt, "Fundamentals of Heat and Mass Transfer", 4th edition, New York, 1995.
[26] A.A. Aleksandrov, 2New International Guidelines for the Thermodynamic Properties of Water and Steam", J. Thermal Engineering, 1998, Vol. 45, No. 9, p. 717.
[27] A.A. Samarskii, V.A.Galaktionov, S.P. Kurdjumov and A.P.Mikhailov, "Blowing-up in the Problems for Quasilinear Parabolic Equations": Moscow, Nauka, 1987.
[28] N.N. Janenko, "The Fractional Step Method for Solution of the Multi-dimensional Problems of Mathematical Physics": Novosibirsk, Nauka, 1967.
[29] D.A. Anderson, J.C. Tannehill and R.H. Pletcher, "Computational Fluid Mechanics and Heat Transfer": New York, McGraw-Hill, 1984.

Ivan V. Kazachkov was born in Alexandriya, Ukraine, in 1954. He is a Mechanical Engineer who had earned his PhD (Candidate of Physical and Mathematical Sciences, 1981) and MSc (1976) from the Kyiv National Taras Shevchenko University and got his Full Doctorship (1991) in Engineering Sciences from the Institute of Physics of the Latvian Academy of Sciences in Riga.

He is Head of Department of Applied Mathematics and Informatics at the Nizhyn State University named after M. Gogol. Also he is Affiliated Professor of the Royal Institute of Technology in Stockholm. Recently during 5 years he was teaching and doing research at the National Technical University of Ukraine "KPI". He has been teaching numerical methods and doing research in modeling of multiphase systems as visiting professor (1999-2004 permanently and afterwards part-time) at the Royal Institute of Technology in Stockholm. He has over 200 publications in scientific journals and conferences, including 5 patents on the methods and devices for metal granulation and 7 books (lecture notes and monographs), e.g. the following:

- Kazachkov I.V. and Kalion V.A. *Numerical continuum mechanics*. Lecture notes.- Stockholm: Royal Institute of Technology.- Vol. 1.- 2nd Ed.- 2008.- 273 pp.
- Kazachkov I.V. and Palm B. *Analysis of Annular Two-phase Flow Dynamics under Heat Transfer Conditions//* J. of Enhanced Heat Transfer. 2005.- 1.- P. 1-22.
- Kolesnichenko A.F., Kazachkov I.V., Vodyanuk V.O. and Lysak N.V. *Capillary MHD Flows with Free Surfaces*, Monograph, Naukova Dumka, Kiev, 1988, 176 pp. (in Russian).

He participates in European research programs and committees. A number of PhD students are doing research under his supervision. The research activities include Parametric Control in Continua, Multiphase Flows, Controlled Film Flow Decay, and Granulation of Metals for Special Metallurgy, Modeling and Simulation.